Lithuanian Journal of Physics, Vol. **50**, No. 3, pp. 335–344 (2010) doi:10.3952/lithjphys.50304

BIOMASS BURNING IMPACT ON BLACK CARBON AEROSOL MASS CONCENTRATION AT A COASTAL SITE: CASE STUDIES

V. Ulevičius, S. Byčenkienė, N. Špirkauskaitė, and S. Kecorius

Center for Physical Sciences and Technology, Savanorių 231, LT-02300 Vilnius, Lithuania
E-mail: ulevicv@ktl.mii.lt

Received 19 March 2010; revised 23 August 2010; accepted 16 September 2010

During 25 March – 5 April 2010 intense wildfires in the Kaliningrad region (Russia) occurred. The resultant smoke plume blanketing the Lithuanian western part was seen in satellite images. Concurrently, an extremely high black carbon (BC) aerosol mass concentration was observed at the background Preila site (55°55′ N, 21°00′ E, 5 m a.s.l., Lithuania). The surface measurements and calculation of Ångström exponent of the absorption coefficient α carried out separately for shorter and longer wavelengths (i. e., λ =370–520 nm and λ =590–950 nm) showed that high levels of BC aerosol were related to the transport of air masses rich in biomass burning products from the Kaliningrad region caused by active grass burning. During this event the BC aerosol mass concentration of 1-hour average reached 13000 ng m^{-3}, while normally annual mean concentration values are about 750 ng m^{-3}. The transport of the burning products from fire areas is associated with southeastern flow and strong advection of warm and dry air from South Europe in the lower troposphere. During the event the highest mean values of Ångström exponent of the absorption coefficient $\alpha_{370-520}$ and $\alpha_{590-950}$ were observed (2.0±0.4 and 1.6±0.3, respectively). The mean values of Ångström exponent of the absorption coefficient during the study period obviously indicate that a major part of carbon mass in aerosol particles transferred by the regional air masses comes from the wildfire location.

Keywords: black carbon aerosol, aethalometer, biomass burning, Ångström exponent of the absorption coefficient

PACS: 92.60.Mt, 92.30.Ef, 92.20.Bk

1. Introduction

The biomass burning has long been recognized as a significant source of reactive species such as aerosol, carbon monoxide (CO), hydrocarbons, and nitrogen oxides (NO_x), which play an important role in the chemistry and radiative budget of the troposphere [1, 2]. During biomass burning periods, the visibility in affected areas can be heavily reduced, and the health effects on the local population can be substantial. Moreover, biomass burning particles are efficient cloud condensation nuclei, they can influence the formation of clouds and affect the Earth's climate by directly scattering and absorbing the atmospheric radiation [3–6]. Along with absorbing aerosols, black carbon (BC) or elemental carbon fraction is known to be most effectively absorbing solar radiation [7, 8].

In Eastern Europe the open biomass burning of agricultural residues and other waste remains a significant issue [9–11]. Smoke aerosols released from biomass fires are a complex of chemical mixture of organic and inorganic materials, simultaneously involving the gaseous, liquid, and solid phases [2, 12–14]. The long-range transport of emissions from wildfires from Ukraine and European part of Russia increases the particular matter concentrations in Eastern and Northern European countries, frequently during spring and summer [15–17]. After emission into the atmosphere, BC is processed by the condensation of secondary material such as sulfates, nitrates, or organic matter increasing the size and hygroscopicity of the particles [18]. During atmospheric ageing, the refractory component of BC is chemically quite stable and thus is relatively invariant, making BC an ideal tracer of primary pollution [19]. Although concentrations of BC are determined permanently at many locations worldwide such as North America [20, 21], South America [22, 23], Africa [24], and the Mediterranean [25], the reports have shown that biomass burning particles found in different regions vary in concentrations. The variety of particle characteristics may be due to several factors such as intensity of fires, moisture, weather conditions, and other variables.

In this work, the regional air mass transport event that occurred in Lithuania on 25 March – 5 April 2010 was investigated. The potential source areas of

ISSN 1648-8504

particles and the presence of open biomass burning were investigated using terrestrial information operationally derived from satellite data including those from NASA's MODIS instrument. Air mass backward trajectories and smoke dispersion modelling data were used to identify the origin and to characterize the regional transport from open biomass burning as a particle source of the atmospheric pollution into a synoptic weather context. The BC aerosol mass concentrations in conjunction with analysis of Ångström exponent of the absorption coefficient were investigated.

2. Methods

2.1. Site description

The black carbon aerosol mass concentration measurements were performed at the Preila environmental pollution research station (55°55′ N, 21°00′ E, 5 m above the sea level) in the coastal/marine environment. This station is located on the Curonian Spit, which separates the Curonian Lagoon and the Baltic Sea, and thus can be characterized as a regionally representative background environment. The Curonian Lagoon, the largest coastal bay in the Baltic Sea, is a highly eutrophied water body. It is an enclosed shallow (mean depth 3.7 m) bay connected to the Baltic Sea by the narrow (400–600 m wide) Klaipėda strait. One of the nearest industrial cities, Klaipėda, is at a distance of about 40 km to the north and the other major city, Kaliningrad (Russia), is 90 km to the south from Preila.

2.2. Fire smoke transport and air mass isentropic backward trajectories

To identify possible events of regional air mass transport, the location of a thermal anomaly was detected with the MODIS sensor using data from the middle infrared and thermal infrared bands [26]. The MODIS monthly fire maps, available since 2001, have shown that these events of biomass burning in March–April occur annually. However, the duration, geographical extent, and emission of the smoke from these fires differ year by year. The results of the Navy Aerosol Analysis and Prediction System (NAAPS) model were used to determine the distribution of smoke aerosols from fires (model description and results are available from the web pages of the Naval Research Laboratory, Monterey, CA, USA; http://www.nrlmry.navy.mil/aerosol/). The NAAPS model has recently been modified to incorporate real-time observations of biomass burning based on the

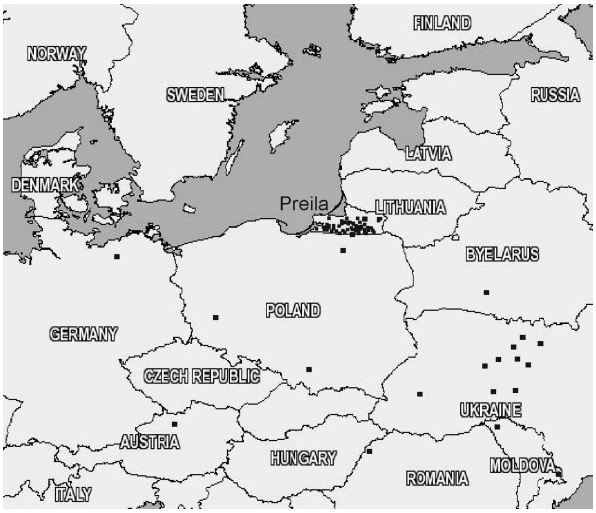

Fig. 1. Locations of the active fires identified from MODIS observations (Europe subset: Terra 1 km true colour image for 3 April 2010).

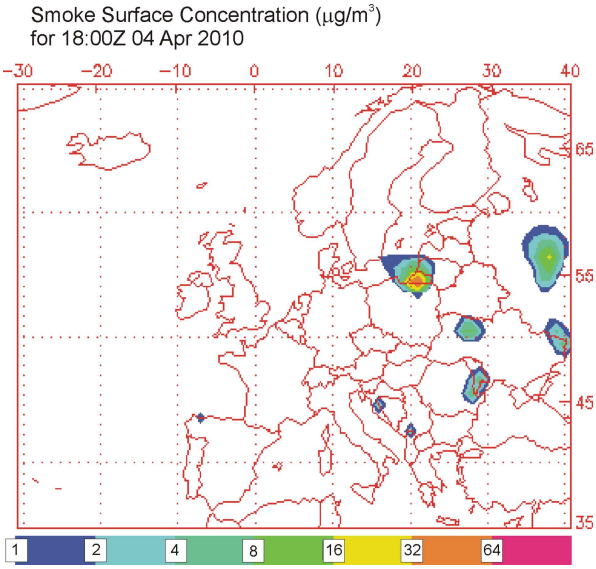

Fig. 2. Smoke mass mixing ratio at the surface by NAAPS.

joint Navy/NASA/NOAA Fire Locating and Modeling of Burning Emissions system (FLAMBE, http://www.nrlmry.navy.mil/flambe/) [27, 28]. The aerosol characteristics with respect to categorized air mass isentropic backward trajectories for initial estimation of the wildfire potential source location and quantitative contribution have been analysed. Air mass isentropic backward trajectories were analysed using the HYbrid Single-Particle Lagrangian Integrated Trajectory (HYSPLIT4) model [29] with the Final Analyses (FNL; 2010) and the Global Data Assimilation System (GDAS) meteorological databases at the NOAA Air Resources Laboratory's web server [30]. The weather and baric topography maps from the European

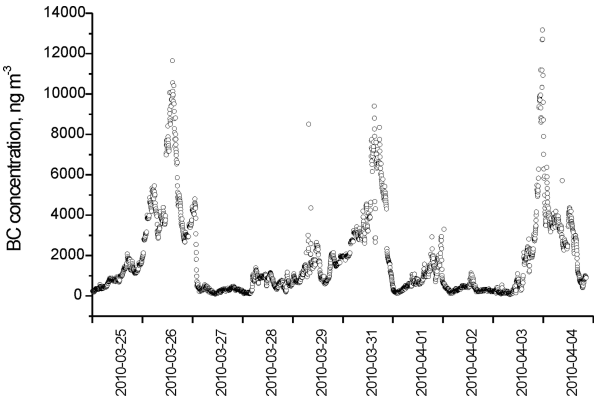

Fig. 3. Time series of BC mass concentration.

Meteorological Bulletin (Germany weather service, http://www.wetterzentrale.de) were analysed.

2.3. Black carbon aerosol mass concentration measurements

A Magee Scientific Co. Aethalometer™, Model AE40 Spectrum, manufactured by Optotek, Slovenia was deployed at the site and provided real-time, continuous measurements of the BC mass concentration. The optical transmission of carbonaceous aerosol particles was measured sequentially at seven wavelengths λ (370, 450, 520, 590, 660, 880, and 950 nm). The concentration of black carbon corresponds to the 880 nm wavelength.

The aethalometer data recorded with a 2-minute time basis were compensated for loading effects using an empirical algorithm [31].

A power law fit is commonly applied to describe the wavelength dependence of absorption coefficient b_{abs}:

$$b_{\mathrm{abs}} \propto \lambda^{-\alpha}\,, \tag{1}$$

where λ is the wavelength and α is the usually called Ångström exponent of the absorption coefficient and is computed by fitting an exponential curve [32]. The wavelength dependence of the light absorption can be better approximated by separate exponential fits of the lower (370–520 nm) and higher (590–950 nm) wavelengths (coefficient of determination $r^2 > 0.99$) obtained by an exponential curve fit over all seven wavelengths.

Spatial and temporal variations of PM2.5 and PM10 within Klaipėda city were investigated using the data sets collected from air quality monitoring site of the Lithuanian Environment Protection Agency. The mass concentrations of PM2.5 and PM10 were obtained with the automatic analyzers using the French Environment S.A model 1M monitors based on the β-attenuation method. The measurements of the carbon monoxide and nitrogen oxides were performed continuously with the Environment S.A model CO11M (infrared gas absorption method) for CO and model AC31M (chemoluminescent method) for NO_x [17].

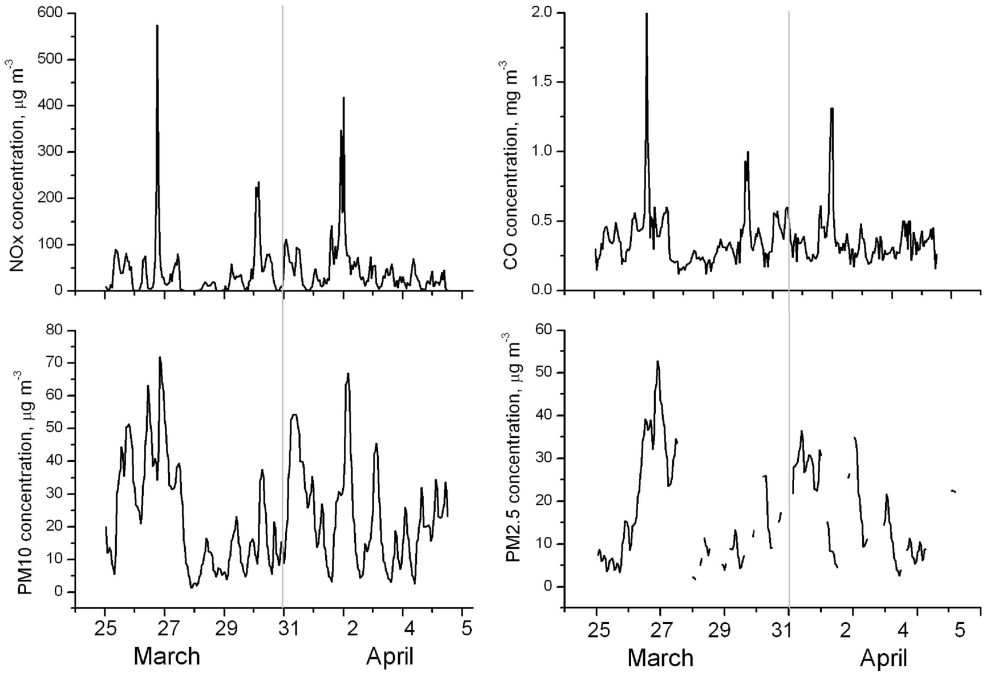

Fig. 4. Time series of NO_x, CO, PM10, and PM2.5 concentration as measured at the Klaipėda AQ station during March–April 2010.

3. Results

3.1. Analysis of high black carbon concentration episodes

In this study we focus on the strongest period of wildfire in the Kaliningrad region that occurred on 25 March – 5 April 2010. They commonly start in March, and the number of fires is largest in April. The intensity of these fires varies from year to year, which is largely caused by meteorological conditions in spring, such as the occurrence of precipitation, the temperature, etc. For example, in Fig. 1 the Fire Mapper – a web mapping interface that displays hotspots/fires detected by the MODIS Rapid Response System – products have provided data about the area and coverage of fires.

Satellite image and smoke dispersion by NAAPS (Fig. 2) suggested substantial emissions and regional transport from the large biomass burning in the Kaliningrad region at that time. During this period territories close to Preila were covered with high BC aerosol mass concentrations that were clear outliers in their respective series, both for hourly concentrations and 24-h means (Fig. 3). Biomass burning products were redistributed over Lithuania by the large-scale atmospheric circulation. As shown in Fig. 1, the MODIS clearly illustrates the fire location. Model forecasts by NAAPS for this period suggested substantial emissions and regional transport of smoke (for smoke, we assume particles of 0.01 μm radius) (Fig. 2) from the large fires burning in the Kaliningrad region at that time.

During the study the NAAPS model predicted the optical depth of 0.4 at a wavelength of 0.55 μm for three components: sulfate, dust, and smoke over the Lithuanian western part due to smoke from the wildfires. It should be mentioned that the measured BC aerosol mass concentration might originate from some other burning region, which was located closer to the site but missed by MODIS, possibly due to clouds.

During this event the BC aerosol mass concentration of 1-hour average reached 13 000 ng m^{-3}, while normally annual mean concentration values are about 750 ng m^{-3} [33]. During the study period on 25 March – 5 April 2010 the urban air quality monitoring station recorded moderate or higher concentrations of PM2.5,

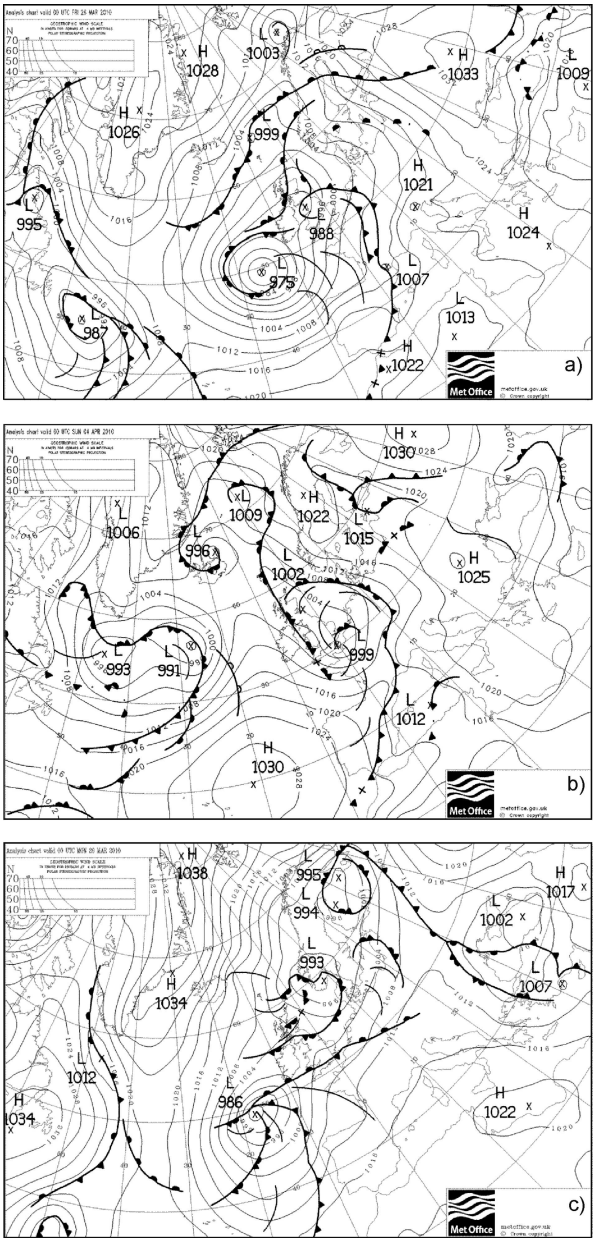

Fig. 5. Weather maps from the European Meteorological Bulletin (Germany Weather Service, http://www.wetterzentrale.de) for 00 UTC (a) 02 Lithuania local wintertime, 26 March; (b) 03 Lithuania local summertime, 29 March; (c) 03 Lithuania local summertime, 4 April 2010.

Table 1. The mean daily meteorological parameters at the Klaipėda (Šilutės motorway) air quality station during the study period (25 March – 5 April 2010).

Days	25	26	27	28	29	30	31	1	2	3	4	5
T, °C	9.2	10.4	3.4	3.8	5.3	8.9	13.5	4.7	4.6	2.8	9.5	5.3
Relative humidity (RH), %	80	72	96	59	91	85	72	86	71	75	74	74
Pressure, hPa	1014	1003	990	1003	1005	1002	999	1013	1015	1016	1015	1020
Wind speed, m·s^{-1}	3.3	1.6	3.2	1.4	0.8	2.5	2.4	0.4	1.3	0.3	2.6	1.0

PM10, NO_x, and CO (Fig. 4). As can be seen from Fig. 4, appreciable increase in the PM10 concentration has been monitored during the course of the pollution event that suggests that a high concentration event has been a widespread regional transport event. A strong CO and NO_x enhancement (from 0.5 to 2 $\mathrm{mg\,m^{-3}}$ and from 100 to 500 $\mu\mathrm{g\,m^{-3}}$, respectively) was observed. Bearing in mind that BC found during pollution events is mainly the product of incomplete combustion of biomass, the relative contribution compared to that from other sources is not certain. The pollution events at the urban site were not influenced only by urban sources but also by biomass burning during early spring [34].

The dispersion of biomass smoke and resulting high concentration events, their severity, duration, and affected areas depend on meteorological conditions. For the current event, the weather maps showed that its exceptionally long duration was caused by a long-lasting anticyclonic system over western Russia, which caused the fire fumes to be transported from the burning region. Strong temporal variations in the course of the BC aerosol mass concentration showed a possible correlation with the change of atmospheric processes resulting in primary carbonaceous aerosol outflow from biomass burning areas in the Kaliningrad region. During 25–26 March, deep cyclone (975 hPa) over the eastern Atlantic Ocean and high pressure (1033 hPa) systems over Russia formed the atmospheric circulation over Lithuania associated with south–eastern flow and strong advection of warm air from South Europe in the lower troposphere (Figs. 5(b), 6). On the next days (27–30 March) low pressure with cold or occluded fronts

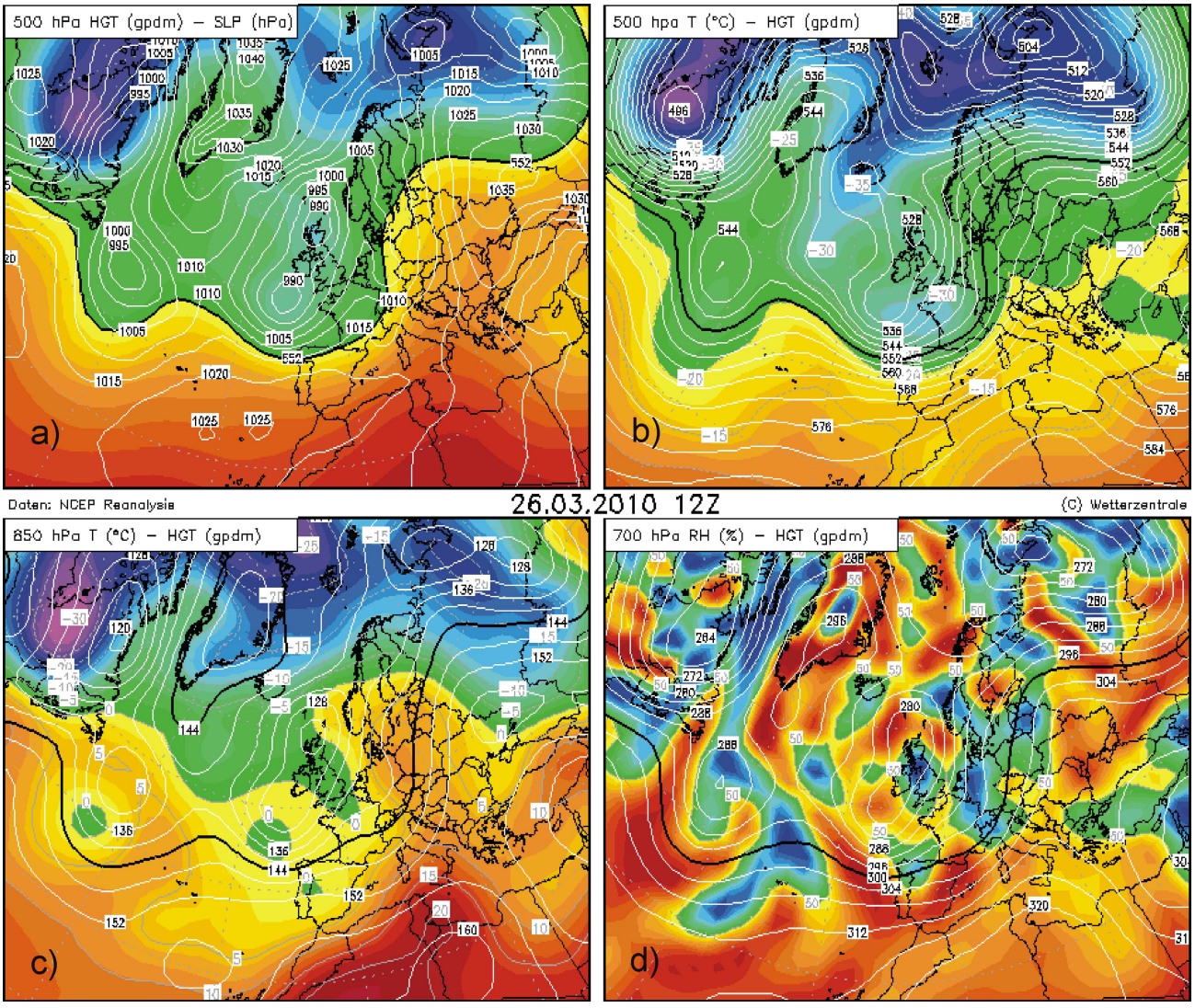

Fig. 6. Baric topographic maps: (a) Absolute topography (AT) 500 hPa above sea level; (b) AT 500 hPa $T\,^{\circ}$C; (c) AT 850 hPa $T\,^{\circ}$C; (d) AT 700 hPa RH % for 26 March 2010 12 UTC.

system and the north–eastern flow transporting polar air masses dominated over the Baltic countries (Fig. 5).

Meteorological data for the study period confirm a significant drop in the temperature (5–7 °C) and an increase in the relative humidity (Table 1).

During these days the BC mass concentration yet again reached the background level (750 ng m^{-3}) (Fig. 3). In all probability, this was related to the passage of cold front with precipitation cleaning the ground level air from biomass burning products at the Preila site and a radical change of air mass advection direction was observed. A sharp increase of the BC mass concentration on 31 March and 4 April (Fig. 3) was clearly associated with a change of the atmospheric circulation type. This was the beginning of wavy several day-long warm and dry air outburst from South-eastern Europe (mainly from Greece) (Figs. 5(c), 7(c)). As seen in Fig. 6(c, d) the tongue of warm and dry air mass extending from Greece to Norway across the Baltic Sea was observed in the lower troposphere because the middle troposphere was covered by the processes of transport of air masses sprawling from northern latitudes. Arrival of the fresh air mass at the study site from south has shown a sudden changing of daily average temperature both on 31 March and 4 April (Table 1). The short-term advection of the air mass has shown the variation of the meteorological parameters since on the next days the transformation of air masses occured.

Analysis of air mass isentropic backward trajectories established the transport of air masses from south over biomass burning areas, especially in lower troposphere

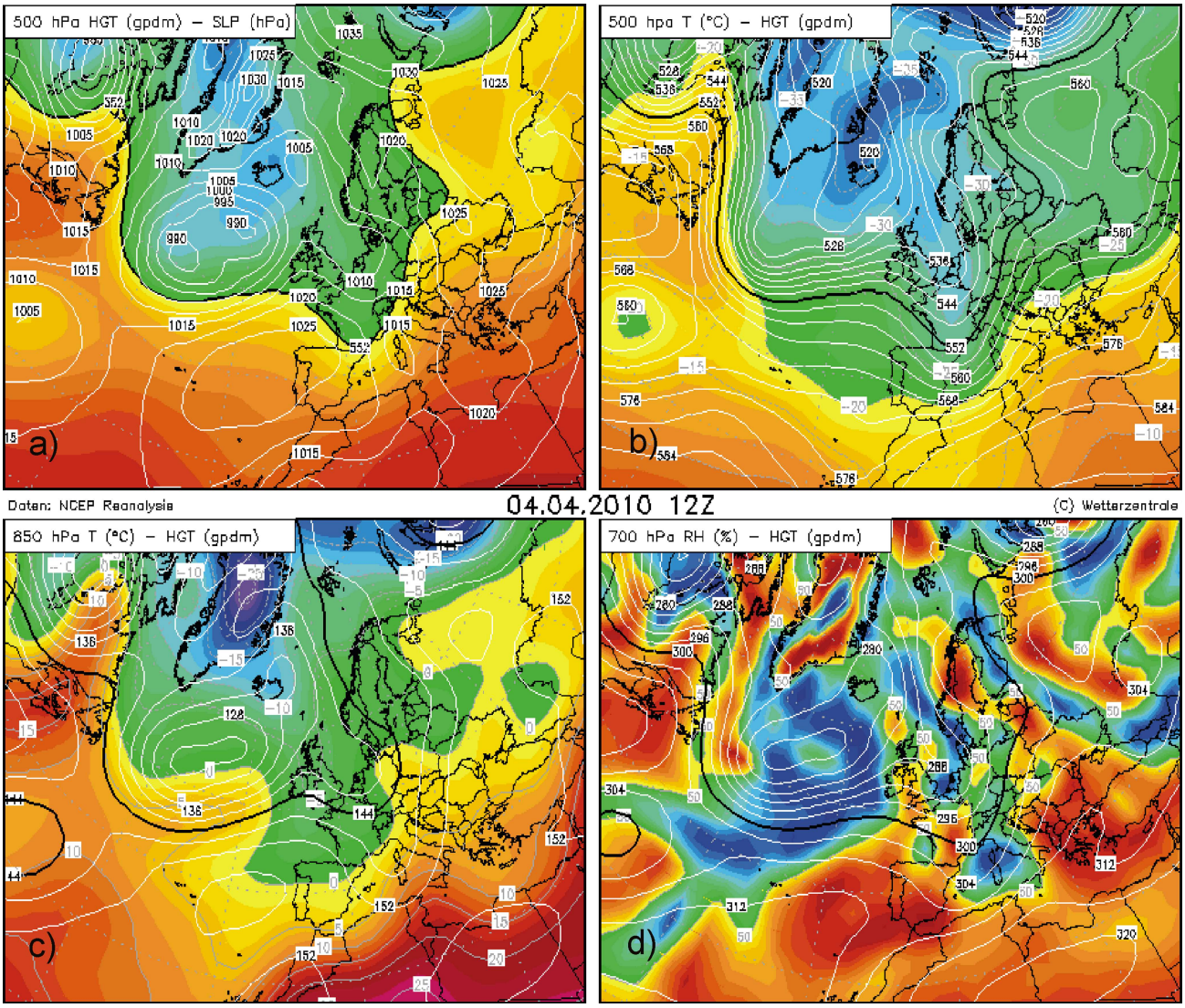

Fig. 7. Baric topographic maps: (a) AT 500 hPa above sea level; (b) AT 500 hPa T °C; (c) AT 850 hPa T °C; (d) AT 700 hPa RH % for 4 April 2010 12 UTC.

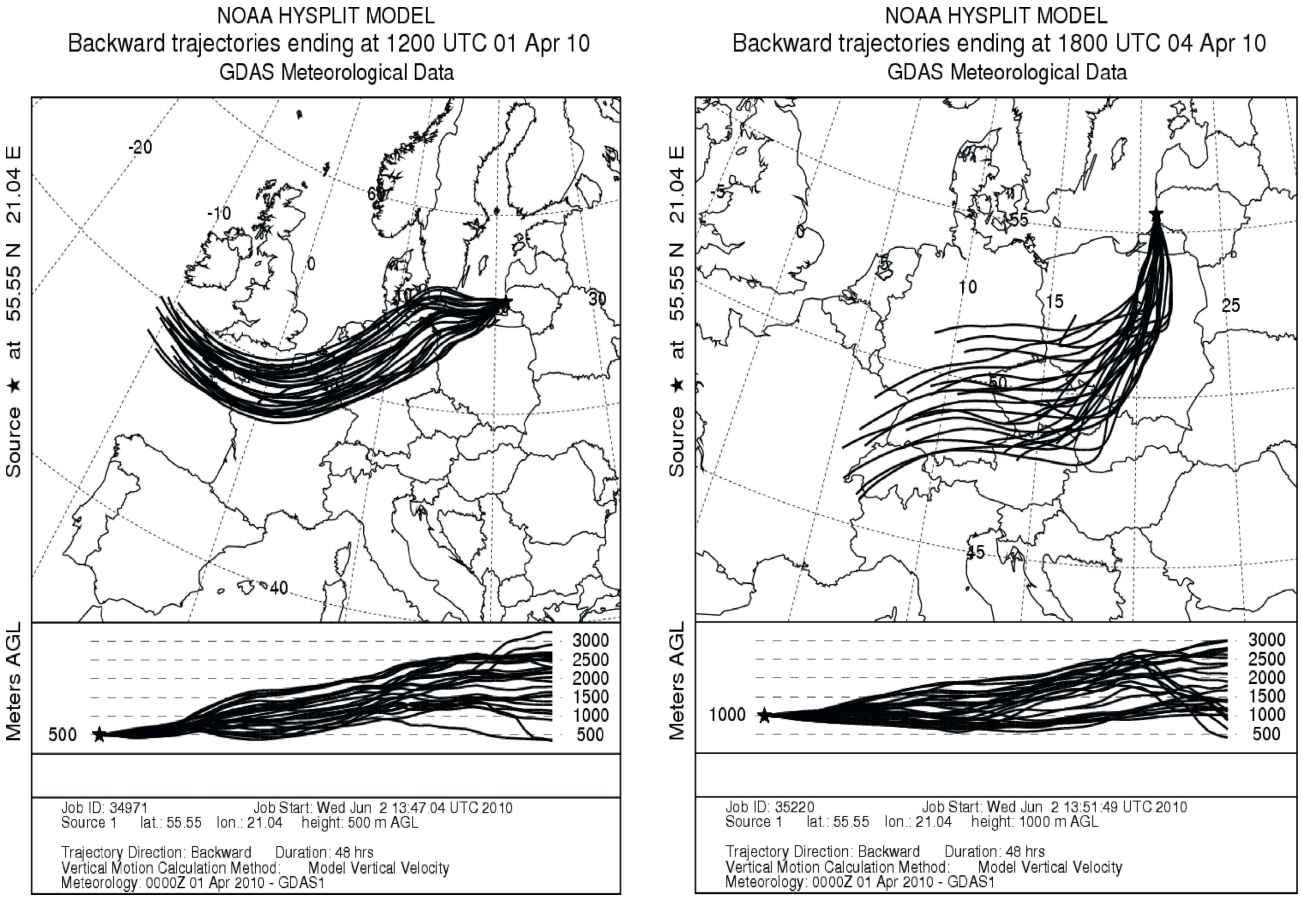

Fig. 8. Air mass regional transport from biomass burning territories in Kaliningrad region on 1 (left panel) and 4 April (right panel) 2010.

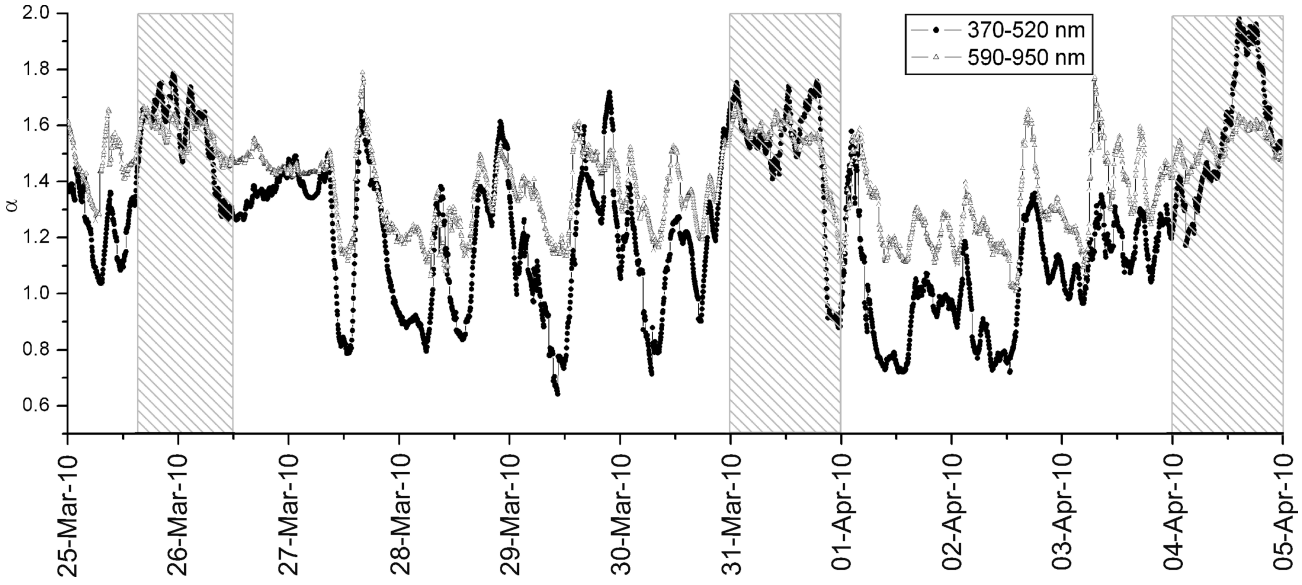

Fig. 9. The light Ångström exponent of the absorption coefficient: $\alpha_{370-520}$ and $\alpha_{590-950}$.

to the north towards the Baltic countries (Fig. 8). The air mass backward trajectory analysis showed that these particles from the Kaliningrad region with air masses were brought to Lithuania and caused three abrupt increases in the BC concentration (Fig. 3).

Moreover, for the study period the site was under the influence of frontal air systems (Fig. 5(b)). The dominant local wind directions were to be either from the north (N) or northeast (NE) (Table 1). It is obvious that during this period polluted air from the biomass burning regions was transported to the site.

3.2. The absorption exponent α as a function of wavelength range

The Ångström exponent of the absorption coefficient was calculated to explain the BC aerosol origin. The Ångström exponents were calculated by fitting b_{abs} for the whole available wavelength intervals: the low wavelength interval 370–520 nm and the high wavelength interval – 590–950 nm (Fig. 9).

The contrast between the events with biomass smoke and those with less smoke is most evident in the short wavelength interval. On 5 April the α values were significantly higher for the shorter wavelengths ($\alpha_{370-520} \approx 2.0 \pm 0.4$) compared to the longer wavelengths ($\alpha_{590-950} \approx 1.6 \pm 0.3$) (Fig. 9). On non-event days, the light absorption coefficients $\alpha_{370-520}$ and $\alpha_{590-950}$ were within a narrow range of 1.2, with weak diurnal cycles. These high values of the absorption exponent are indicative of biomass combustion [32], in our case – wildfires in the Kaliningrad region, as indicated by the air mass isentropic backward trajectory analysis and weather maps. Kirchstetter et al. [35] reported α value of 2.2 for outdoor firewood burning, 1.8 for a savanna fire, and 0.8–1.1 for traffic-dominated sites. Schnaiter et al. [36, 37] reported α value of 1.1 for uncoated diesel soot (measurements with $\lambda = 450$, 550, and 700 nm). Previous investigations showed that the type of wood being burned also influenced the α value as shown by Day et al. [38] where they measured fresh wood smoke from seven types of forest wood with an aethalometer ($\lambda = 370$–950 nm) and reported α values between 0.9 and 2.2.

4. Summary and conclusions

A combination of ground-based and satellite observations was used in this study to investigate different sources of the high black carbon aerosol mass concentration over Lithuanian western part on 25 March – 5 April 2010. During this period the measured black carbon concentration 1-hour average of 13 000 ng m^{-3} exceeded previously established mean values of 750 ng m^{-3}. During the open biomass fire events in the neighbourhood of Lithuania under specific weather conditions the abrupt increases of the BC concentration in the ground level air at the Preila site were observed. Transport of the burning products from fire areas is associated with southeastern flow and strong advection of warm and dry air from South Europe in the lower troposphere. During the event in 2010 the highest mean values of Ångström exponent of the absorption coefficient $\alpha_{370-520}$ and $\alpha_{590-950}$ were observed (2.0 ± 0.4 and 1.6 ± 0.3, respectively). The highest values were comparable to research studies on wood smoke, i. e., $\sim$2. This confirms the infuence of the relative contribution of wood burning on the Ångström exponent of the absorption coefficient α. Observation data from other countries demonstrate that particulate matter levels have been increasing in northern Europe and Scandinavia during spring periods, indicating that these were long-range transport pollution events.

Acknowledgements

This work was partially supported by FP6 project EUSAAR and FP7 project TRANSPHORM.

References

[1] P.J. Crutzen and M.O. Andreae, Biomass burning in the tropics: Impact on atmospheric chemistry and biogeochemical cycles, Science **250**, 1669–1678 (1990).

[2] M.O. Andreae and P. Merlet, Emission of trace gases and aerosols from biomass burning, Global Biogeochem. Cycles **15**, 955–966 (2001).

[3] J.E. Penner, X.Q. Dong, and Y. Chen, Observational evidence of a change in radiative forcing due to the indirect aerosol effect, Nature **427**, 231–234 (2004).

[4] J.S. Reid, T.F. Eck, S.A. Christopher, R. Koppmann, O. Dubovik, D.P. Eleuterio, B.N. Holben, E.A. Reid, and J. Zhang, A review of biomass burning emissions, part III: intensive optical properties of biomass burning particles, Atmos. Chem. Phys. **5**, 827–849 (2005).

[5] D. Rose, A. Nowak, P. Achtert, A. Wiedensohler, M. Hu, M. Shao, Y. Zhang, M.O. Andreae, and U. Poschl, Cloud condensation nuclei in polluted air and biomass burning smoke near the mega-city Guangzhou, China – Part 1: Size-resolved measurements and implications for the modeling of aerosol particle hygroscopicity and CCN activity, Atmos. Chem. Phys. Discuss. **8**, 17343–17392 (2008).

[6] P. Reutter, H. Su, J. Trentmann, M. Simmel, D. Rose, S.S. Gunthe, H. Wernli, M.O. Andreae, and U. Poschl, Aerosol- and updraft-limited regimes of cloud droplet formation: influence of particle number, size and hygroscopicity on the activation of cloud condensation nuclei (CCN), Atmos. Chem. Phys. **9**, 7067–7080 (2009).

[7] T.L. Anderson, R.J. Charlson, S.E. Schwartz, R. Knutti, O. Boucher, H. Rodhe, and J. Heintzenberg, Climate forcing by aerosols – a hazy picture, Science **300**, 1103–1104 (2007).

[8] V. Ramanathan and G. Carmichael, Global and regional climate changes due to black carbon, Nat. Geosci. **1** (4), 221–227 (2008).

[9] R. Damoah, N. Spichtinger, C. Forster, P. James, I. Mattis, U. Wandinger, S. Beirle, and A. Stohl, Around the world in 17 days – hemispheric-scale transport of forest fire smoke from Russia in May 2003, Atmos. Chem. Phys. **4**, 1311–1321 (2004).

[10] J.V. Niemi, H. Tervahattu, H. Vehkamäki, M. Kulmala, T. Koskentalo, M. Sillanpää, and M. Rantamäki, Characterization and source identification of a fine particle episode in Finland, Atmos. Environ. **38**, 5003–5012 (2004).

[11] J.V. Niemi, H. Tervahattu, H. Vehkamäki, J. Martikainen, L. Laakso, M. Kulmala, P. Aarnio, T. Koskental, M. Sillanpää, and U. Makkonen, Characterisation of aerosol particle episodes in Finland caused by wildfires in Eastern Europe, Atmos. Chem. Phys. **5**, 2299–2310 (2005).

[12] P.A. Simmonds, R. Manning, P. Derwent, M. Ciais, V. Ramonet, V. Kazan, and D. Ryall, A burning question: Can recent growth rate anomalies in the greenhouse gases be attributed to large-scale biomass burning events? Atmos. Environ. **39**, 2513–2517 (2005).

[13] Y.J. Kaufman, D. Tanré, and O. Boucher, A satellite view of aerosols in the climate system, Nature **419**, 215–223 (2002).

[14] H. Huntrieser, J. Heland, H. Schlager, C. Forster, A. Stohl, H. Aufmhoff, F. Arnold, H.E. Scheel, M. Campana, S. Gilge, R. Eixmann, and O. Cooper, Intercontinental air pollution transport from North America to Europe: Experimental evidence from airborne measurements and surface observations, J. Geophys. Res. **110**, D01305 (2005).

[15] M. Sillanpää, A. Frey, R. Hillamo, A.S. Pennanen, and R.O. Salonen, Organic, elemental and inorganic carbon in particulate matter of six urban environments in Europe, Atmos. Chem. Phys. **5**, 2869–2879 (2005).

[16] S. Saarikoski, M. Sillanpää, M. Sofiev, H. Timonen, K. Saarnio, K. Teinilä, A. Karppinen, J. Kukkonen, and R. Hillamo, Chemical composition of aerosols during a major biomass burning episode over northern Europe in spring 2006: experimental and modelling assessments, Atmos. Environ. **41**, 3577–3589 (2007).

[17] V. Ulevičius, S. Byčenkienė, V. Remeikis, A. Garbaras, S. Kecorius, J. Andriejauskienė, D. Jasinevičienė, and G. Mocnik, Characterization of pollution events in the East Baltic region affected by regional biomass fire emissions, Atmos. Res. (2010) [in press].

[18] U. Dusek, G.P. Frank, L. Hildebrandt, J. Curtius, J. Schneider, S. Walter, D. Chand, F. Drewnick, S. Hings, D. Jung, S. Borrmann, and M.O. Andreae, Size matters more than chemistry for cloud-nucleating ability of aerosol particles, Science **312**, 1375–1378 (2006).

[19] M. Kendall, R.S. Hamilton, J. Watt, and I.D. Williams, Characterisation of selected speciated organic compounds associated with particulate matter in London, Atmos. Environ. **35**, 2483–2495 (2001).

[20] O. Dubovik, B. Holben, T.F. Eck, A. Smirnov, Y.J. Kaufman, M.D. King, D. Tanre, and I. Slutsker, Variability of absorption and optical properties of key aerosol types observed in worldwide locations, J. Atmos. Sci. **59**, 590–608 (2002).

[21] T.F. Eck, B.N. Holben, D.E. Ward, M.M. Mukelabai, O. Dubovik, A. Smirnov, J.S. Schafer, N.C. Hsu, S.J. Piketh, A. Qeface, J.L. Roux, R.J. Swap, and I. Slutsker, Variability of biomass burning aerosol optical characteristics in southern Africa during the SAFARI 2000 dry season campaign and a comparison of single scattering albedo estimates from radiometric measurements, J. Geophys. Res. Atmos. **108**(D13), 8477 (2003).

[22] B.E. Anderson, W.B. Grant, G.L. Gregory, E.V. Browell, J.E.C. Jr., G.W. Sachse, D.R. Bagwell, C.H. Hudgins, and D.R. Blake, Aerosols from biomass burning over the tropical South Atlantic region: Distributions and impacts, J. Geophys. Res. **101**, 24117–24137 (1996).

[23] F. Echalar, P. Artaxo, J.V. Martins, M. Yamasoe, and F. Gerab, Long-term monitoring of atmospheric aerosols in the Amazon Basin: Source identification and apportionment, J. Geophys. Res. **103**(31), 849–864 (1998).

[24] J. Haywood, S. Osborne, P. Francis, A. Keil, P. Formenti, M.O. Andreae, and P.H. Kaye, The mean physical and optical properties of regional haze dominated by biomass burning aerosol measured from the C-130 aircraft during SAFARI 2000, J. Geophys. Res. Atmos. **108**(D13), 8473 (2003).

[25] P. Formenti, O. Boucher, T. Reiner, D. Sprung, M.O. Andreae, M. Wendisch, H. Wex, D. Kindred, M. Tzortziou, A. Vasaras, and C. Zerefos, STAAARTE-MED 1998 summer airborne measurements over the Aegean Sea 2. Aerosol scattering and absorption, and radiative calculations, J. Geophys. Res. Atmos. **107**(D21), 4551 (2002).

[26] L. Giglio, Characterization of the tropical diurnal fire cycle using VIRS and MODIS observations, Remote Sens. Environ. **108**, 407–421 (2007).

[27] J.S. Reid, E.M. Prins, D.L. Westphal, C.C. Schmidt, K.A. Richardson, S.A. Christopher, T.F. Eck, E.A. Reid, C.A. Curtis, and J.P. Hoffman, Real-time monitoring of South American smoke particle emissions and transport using a coupled remote sensing/box-model approach, Geophys. Res. Lett. **31**, L06107 (2004).

[28] R. Honrath, R.C. Owen, M. Val Martin, J.S. Reid, K. Lapina, P. Fialho, M.P. Dziobak, J. Kleissl, and D.L. Westphal, Regional and hemispheric impacts of anthropogenic and biomass burning emissions on summertime CO and O_3 in the North Atlantic lower free troposphere, J. Geophys. Res. Atmos. **109**(D), D24310 (2004).

[29] R.R. Draxler and G.D. Rolph, *HYSPLIT (HYbrid Single-Particle Lagrangian Integrated Trajectory) Model access via NOAA ARL READY Website* http://ready.arl.noaa.gov/HYSPLIT.php (NOAA Air Resources Laboratory, Silver Spring, MD, 2003).

[30] G.D. Rolph, *Real-time Environmental Applications and Display sYstem (READY) Website* http://ready.arl.noaa.gov (NOAA Air Resources Laboratory, Silver Spring, MD, 2010).

[31] A. Virkkula, T. Mäkelä, R. Hillamo, T. Yli-Tuomi, A. Hirsikko, K. Hämeri, and I.K. Koponen, A simple procedure for correcting loading effects of aethalometer data, J. Air Waste Manag. Assoc. **57**, 1214–1222 (2007).

[32] J. Sandradewi, A.S.H. Prévôt, E. Weingartner, R. Schmidhauser, M. Gysel, and U. Baltensperger, A study of wood burning and traffic aerosols in an Alpine valley using a multi-wavelength Aethalometer, Atmos. Environ. **42**, 101–112 (2008).

[33] J. Andriejauskienė, V. Ulevičius, M. Bizjak, N. Špirkauskaitė, and S. Byčenkienė, Black carbon aerosol at the background site in the coastal zone of the Baltic Sea, Lith. J. Phys. **48**, 183–194 (2008).

[34] A. Garbaras, J. Andriejauskienė, R. Barisevičiūtė, and V. Remeikis, Tracing of atmospheric aerosol sources using stable carbon isotopes, Lith. J. Phys. **48**, 259–264 (2008).

[35] T.W. Kirchstetter, T. Novakov, and P.V. Hobbs, Evidence that the spectral dependence of light absorption by aerosols is affected by organic carbon, J. Geophys. Res. Atmos. **109**, D21208 (2004).

[36] M. Schnaiter, H. Horvath, O. Möhler, K.H. Naumann, H. Saafhoff, and O.W. Schock, UV–VIS–NIR spectral optical properties of soot and soot-containing aerosols, J. Aerosol Sci. **34**, 1421–1444 (2003).

[37] M. Schnaiter, C. Linke, O. Möhler, K.H. Naumann, H. Saathoff, R. Wagner, U. Schurath, and B. Wehner, Absorption amplification of black carbon internally mixed with secondary organic aerosols. J. Geophys. Res. Atmos. **110**, D19204 (2005).

[38] D.E. Day, J.L. Hand, C.M. Carrico, G. Engling, and W.C. Malm, Humidification factors from laboratory studies of fresh smoke from biomass fuels, J. Geophys. Res. Atmos. **111**, D22202 (2006).

BIOMASĖS DEGINIMO ĮTAKA JUODOSIOS ANGLIES AEROZOLIO MASĖS KONCENTRACIJAI JŪROS PAKRANTĖJE: ATVEJO ANALIZĖ

V. Ulevičius, S. Byčenkienė, N. Špirkauskaitė, S. Kecorius

Fizinių ir technologijos mokslų centras, Vilnius, Lietuva

Santrauka

Tirtas juodosios anglies aerozolio masės koncentracijos padidėjimas Lietuvos pajūryje tolimosios pernašos metu iš gaisrų apimtų teritorijų Kaliningrado srityje 2010 metų kovo 25 – balandžio 5 dienomis. Didelis išmetamų teršalų iš gaisrų apimtų teritorijų kiekis sukūrė dūmų šleifą, nusidriekusį link Lietuvos jūros pakrantės. Tuo metu Preilos aplinkos užterštumo tyrimų stotyje buvo stebėta didelė juodosios anglies aerozolio masės koncentracija. Tyrimų metu Preiloje juodosios anglies vidutinė valandos masės koncentracija siekė 13000 ng m^{-3}, kai vidutinė metinė vertė siekia 750 ng m^{-3}. Teršalų koncentracijos matavimai ir sugerties koeficiento Angstremo eksponentės α analizė, atlikta atskirai trumpų ir ilgų bangų diapazonuose (t. y. λ = 370–520 ir 590–950 nm), patvirtino, kad didelė juodosios anglies aerozolio masės koncentracija buvo susijusi su biomasės degimo produktų pernaša iš Kaliningrado srities aktyvių gaisrų židinių. Nustatytos didžiausios vidutinės sugerties koeficiento Angstremo eksponentės vertės $\alpha_{370-520}$ ir $\alpha_{590-950}$ siekė atitinkamai 2,0±0,4 ir 1,6±0,3. Siejant juodosios anglies aerozolio koncentracijos kaitą su atmosferos cirkuliacija nustatyta, kad didžiausia koncentracija buvo susijusi su pietryčių srautu ir stipria šilto ir sauso oro advekcija į Lietuvos pajūrį iš Pietų Europos.